Proceedings of the National Conference
On Undergraduate Research (NCUR) 2014
University of Kentucky, Lexington, KY
April 3-5, 2014

Particle-in-cell Simulations of Inverse Compton Scattering

Jamison Thorne
Department of Physics
Northern Illinois University
DeKalb IL 60115, USA

Faculty Advisors: Dr. Philippe R.-G. Piot

Abstract

Producing high-quality x rays within a compact footprint could have important applications for high-precision medical imaging and national security. A method consisting in reflecting a short-pulse laser onto a "relativistic mirror" (a moving sheet of electrons) has been proposed and recently demonstrated. The purpose of this project is to carry some numerical simulation to eventually investigate possible manipulations of the laser and electron-beam shapes that could lead to substantial improvement of the X ray's production. In this paper we present the development of a particle-in-cell model and its benchmarking with theory.

Keywords: Electron Beam, Coherent Light Source, Electrodynamics

1. Background

In inverse Compton scattering (ICS) an electromagnetic wave with frequency ω_L is scattered off a moving electron [1]. In this process the frequency of the wave is upshifted; see Fig. 1. When the electron and electromagnetic wave collide head on, part of the wave is backscattered and it final frequency is upshifted to

$$\omega = 4\gamma^2\omega_L\left(\frac{1}{1+\frac{a_0^2}{2}}\right), \quad (1)$$

where γ is the electron's Lorentz factor defined as the ratio of the electron total energy to its rest mass, and $a_0$is the laser normalized potential defined as $a_0 \equiv \lambda_L\hat{E}/(2\pi mc^2)$ where $e,\ \lambda_L \equiv 2\pi c/\omega_L,\ \hat{E}$, and mc^2 are respectively the electronic charge, the incoming wave wavelength and peak electric field, and the rest mass of the electron. The values of $a_0 \gg 1$ and $a_0 \ll 1$ corresponds to relativistic and non-relativistic intensities respectively.

The latter equation demonstrates the main advantage of the ICS process to produce short-wavelength, e.g., X-ray radiation. For instance, colliding a 5-MeV electron beam ($\gamma = 10$) head-on with an 800-nm (ω_L=2.3 PHz) laser pulse commercially available enable the production of hard x rays with ω=942.5 PHz corresponding to a wavelength of 2 nm in the soft X-ray regime (here we assume a_0 to be very small and neglect its contribution in Eq. 1). Another advantage of the ICS-based radiation source is its ability to tune the frequency of the output radiation by simply changing the electron energies. Therefore ICS could pave the road toward the development of a very compact X-ray sources that could be used toward a vast range of applications including industry, medicine, homeland security and fundamental science. The efficiency of the ICS process is relatively small 10^{-4} and one way to improve this limitation is to have the electron within the bunch emitted radiation in phase so that it is coherently enhanced [2].

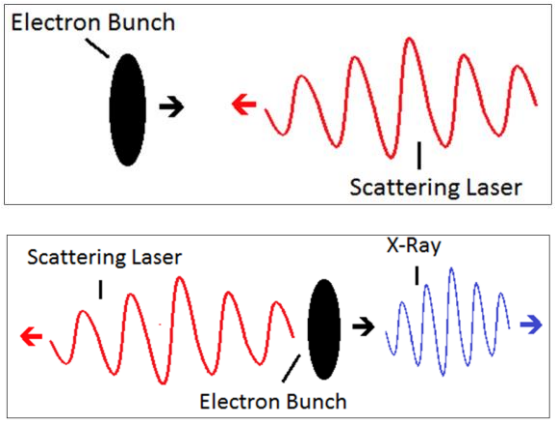

Figure 1. Schematics of the head-on inverse Compton scattering (ICS): an electron bunch (black ellipse) and laser pulse (red trace) collide (top diagram). After collision (bottom diagram) a short-wavelength (possibly x-ray) pulse is produced and co-propagates along the same direction as the electron bunch.

2. Modeling methodology

In practice, when colliding an electron beam with a laser pulse an analytical prediction of the property of the scattered pulse is not possible and one usually relies on semi-analytical approach [3]. Since our ultimate goal is to eventually develop a model that could also be used to investigate and optimize the production of coherently enhanced radiation, we focus on developing a model that works from "first principles".

Developing such a model is computationally challenging. First, the electron beam under consideration generally consists of a large number (10^8) of electrons each following their own trajectory. Second, the laser pulse cannot be modeled by a simple plane wave but need to be described using a realistic field amplitude and transverse distribution. Therefore, to precisely understand the dynamics of the electrons in the field of the laser pulse, numerical simulations based on finite-different time-domain (FDTD) technique is used. We implement the model within the WARP open-source framework available from Lawrence Berkeley National Laboratory, which is capable of solving first principle arbitrary electrodynamics problems [4]. The electromagnetic solver uses a fine-difference time-domain technique to solve Maxwell's equation within a three-dimensional domain with a set of given boundary condition and evolve the system in time. A computational domain is defined and meshed. When particles are added to the system their dynamics is computed via an interpolation of the external field at the particles' locations necessary to compute the Lorentz force experienced by the particle. The field produced by the particles themselves can also be computed using a particle-in-cell scheme (PIC). In the PIC algorithm the particle are "deposited" on three-dimensional mesh discretizing the computational domain and the corresponding charge and current densities are used to solve the non-homogeneous Maxwell's equation. The model takes advantage of a capability of WARP to work in an arbitrary user-specified frame of reference.

To speed up the PIC calculations a Lorentz-Boosted frame was chosen, using the properties of space contraction and time dilation of special relativity gives way to fewer computer operations [5]. In the Lorentz-Boosted frame taken to be the reference frame of the electron bunch (where the bunch is at rest), the laser collides with the stationary bunch and partially reflects off the bunch. In the electron-bunch reference frame the incident laser has a contracted wavelength $\lambda_L' = \lambda_L/[(1+\beta)\gamma]$ (where $\beta \equiv v/c$ with v being the electron-bunch velocity) compared to its wavelength λ_L in the laboratory frame (therefore the laser appears a darker blue in the electron-bunch reference frame). The fraction of the laser reflected off the bunch propagates backward in the Lorentz-boosted frame and its wavelength is also λ_L'.

Therefore, the WARP simulations are carried in the Lorentz boosted frame; see Fig. 2 (top density plot), and upon execution the fields are transformed into the laboratory frame; see Fig. 2 (bottom density plot). In this Lorentz-transformation process the incident laser recovers its laboratory-frame wavelength λ_L, while the backscattered laser has its wavelength in the laboratory frame given by

$$\lambda = \frac{\lambda_L'}{(1+\beta)\gamma} = \frac{\lambda_L}{(1+\beta)^2\gamma^2} \xrightarrow{\beta\simeq 1} \frac{\lambda_L}{4\gamma^2}, \tag{2}$$

which recovers Eq. 1 in the limit of small a_0 and relativistic bunch $\beta \simeq 1$. For WARP, Python was used which is an open-source scripting language. A preliminary numerical model was implemented in WARP by NIU graduate student Ivan Viti with collaboration from Jean-Luc Vay and David Grote from Lawrence Berkeley National Laboratory. Finally, the concept of Fast-Fourier Transforms was used to analyze the simulated electromagnetic fields.

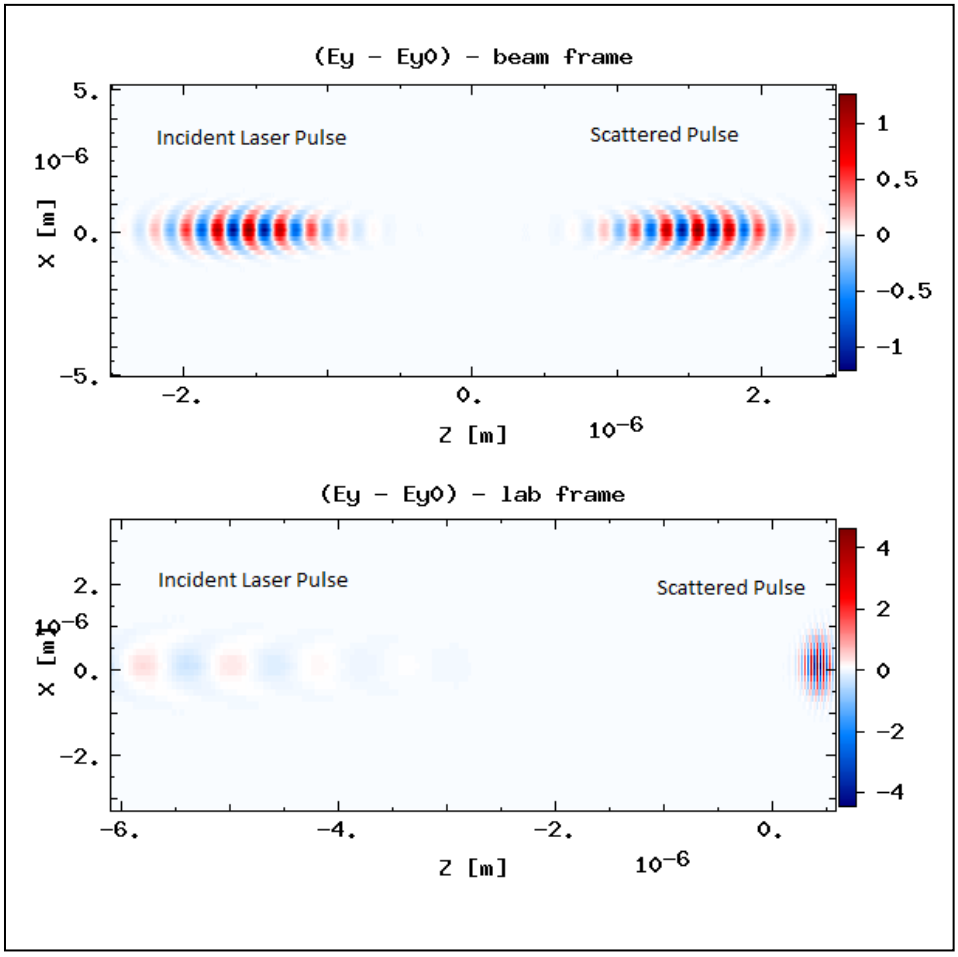

Figure 2. Electric field amplitude after interaction with the electron bunch (not shown) in the Lorentz-boosted (top) and laboratory (bottom) frames. The collision occurs at $z = 0$. The field amplitudes are shown in a slice of the computation domain corresponding to $y = 0$.

3. Warp Framework & Benchmarking

Since we are interested in analyzing the properties of the backscattered pulse, the results presented in Fig. 2 (bottom) needs to be further processed. For our analysis, we use python scripts to extract only the backscattered pulse on the 3-D region of interest within the computational domain. Given the electromagnetic field on a 3-D subspace, we perform fast Fourier transform (FFT) to extract the radiation spectrum.

Figures 3 and 4 present the corresponding results. The FFT for different vertical offset (on Fig. 2) provide the spectrum dependence as function of observation angle as depicts by the density plots appearing at the bottom of these figures. At low normalized vector potential shown in Fig. 3, the on-axis spectrum is quasi monochromatic as shown on the top plots

of Fig. 3. The location of the peak intensity happens at normalized frequency $\frac{\omega}{\omega_0} \simeq 1$ where $\omega_0 \equiv \omega_L/(4\gamma^2)$ as expected from Eq. 1. Additionally, the associated angular-spectral distribution (bottom density plots in Fig. 3) displays a quadratic dependency on $\frac{\omega}{\omega_0}$. This is due to red shifting occurring as one observed the radiation off axis.

Finally in the case of larger normalized vector potential, the spectral content of the radiation extend to much high frequency and the maximum intensity is shifted to $\frac{\omega}{\omega_0} < 1$ values. This is the regime of nonlinear ICS. In this regime, the laser intensity is so high that it drastically impacts the motion of the electrons within the bunch so that the electrons radiate wider-band radiation.

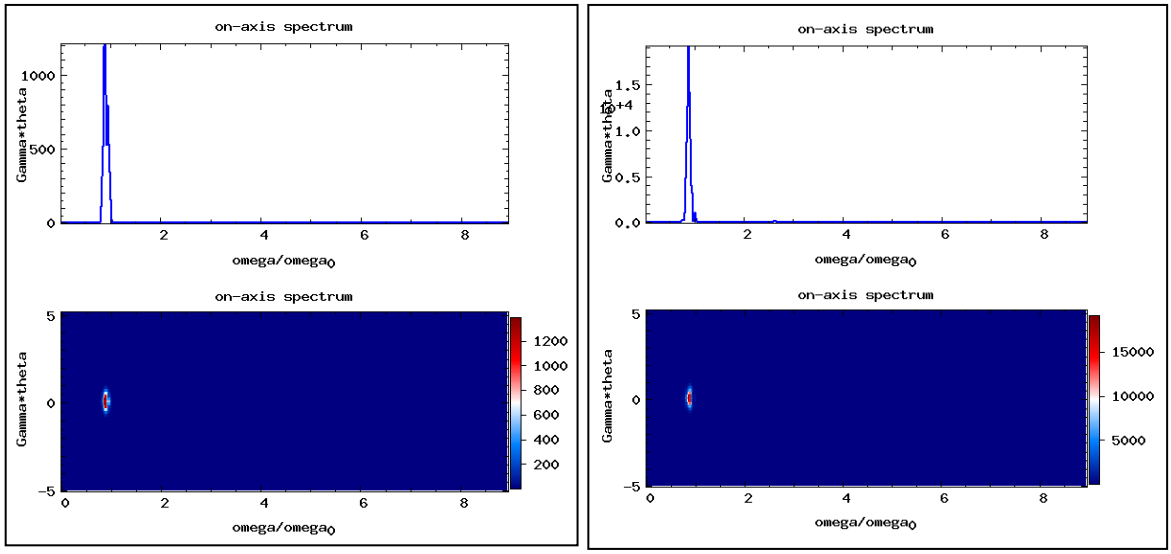

Figure 3. Angular-spectral distribution (density plots) and on axis spectrum (top plots) of the ICS backscattered pulse. The simulations are performed for $a_0 = 0.003$. The left and right panel corresponds respectively to $\gamma = 5$ and 10. The angle θ is defined the angle of observation with respect to the electron beam direction.

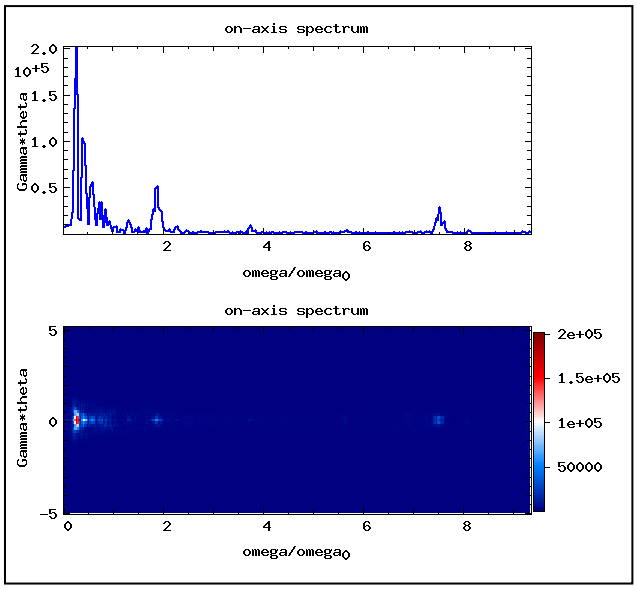

Figure 4. Angular-spectral distribution (density plots) and on axis spectrum (tops plots) of the ICS backscattered pulse. The simulations are performed for $a_0 = 0.3$ and $= 5$. The angle θ is defined the angle of observation with respect to the electron beam direction.

Figures 3 and 4 indicate that the simulations produce results that are in qualitative agreement with the theory. To gain further insight we scan the normalized vector potential and Lorentz factor and record the frequency location of the peak intensity. The results appear in Fig. 5 and confirm that the WARP model quantitatively agree with 1% with the analytical results.

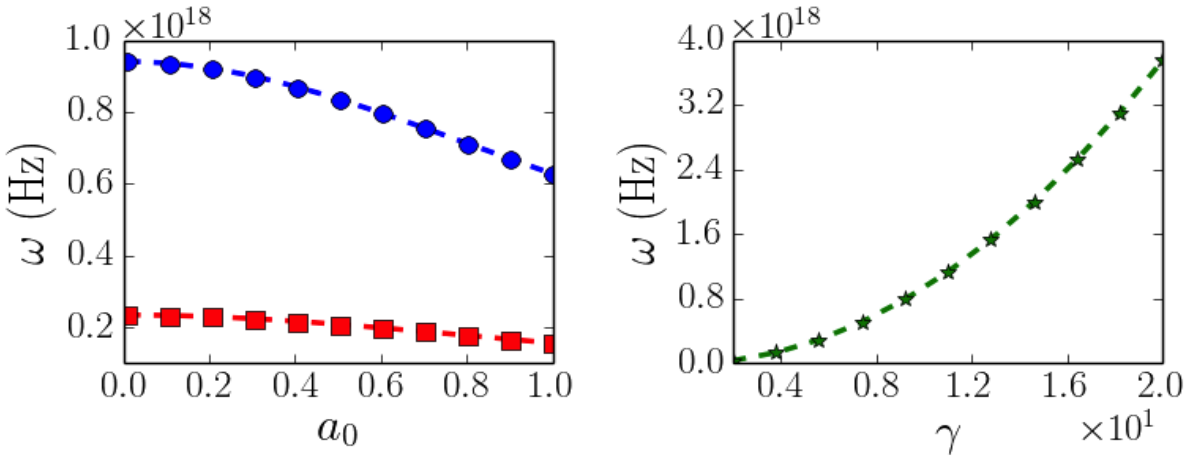

Figure 5. Benchmarking of simulated backscattered radiation as function of the laser pulse normalized vector potential (left plot) and electron bunch Lorentz factor (right). In the left plots the blue and red symbols corresponds to WARP simulation carried for $\gamma = 5$ and $\gamma = 20$. The dashed line are analytical calculation while the symbols correspond to WARP simulations.

4. Conclusion and Future Work

In conclusion, a particle-in-cell model of inverse Compton scattering was successfully implemented in the particle-in-cell program WARP. The simulated results obtained from WARP were benchmarked against the theoretical expectations and quantitatively agree. The onset of nonlinear inverse Compton scattering was also observed for large values of the laser normalized vector potential a_0.

Forthcoming work includes the implementation of shaped electron-bunch distributions necessary to enhance the performances of ICS via emission of coherent radiation.

5. Acknowledgments

The initial development of the model for the ICS process in WARP was carried by a former NIU graduate student, Ivan Viti, in collaboration with Dr. Jean-Luc Vay and Dr. David Grote from Lawrence Berkeley National Laboratory. This work was supported by the Defense Advanced Research Project Agency Grant N66001-11-1-4192 with the Massachusetts Institute of Technology. Special thanks to OSEEL, Northern Illinois University, and my mentor Philippe Piot without whom this work would not have been possible.

6. References

[1] E. S. Sarachik and G. T. Schappert, "Classical Theory of the Scattering of Intense Laser Radiation by Free Electrons", Phys. Rev. D **1**, 2738 (1970)

[2] W. S. Graves, F. X. Kaertner, D. E. Moncton, and P. Piot, "Intense Superradiant X Rays from a Compact Source Using a Nanocathode Array and Emittance Exchange", Phys. Rev. Lett. **108**, 263904 (2012).

[3] Esarey, S. K. Ride, P. Sprangle. "Nonlinear Thomson scattering of intense laser pulses from beams and plasmas", Phys Rev E **48**, 3003 (1993).

[4] J. L. Vay, D. P. Grote, R. H. Cohen, and A. Friedman, "Novel Methods in the Particle-In-Cell Accelerator Code-Framework Warp" Comput. Sci. Disc. **5** 014019 (2012).
[5] J.-L. Vay, "Noninvariance of space-and-time-scale ranges under a Lorentz transformation and the implication to the study of relativistic interactions", Phys. Rev. Lett **98**, 130405 (2007); see also Phys. Rev. Focus **19**, 10 (2007).
[6] I. Viti, "Summary of Achievements Using WARP", unpublished internal note (2013).